

NEW NOVEL METHOD TO ESTIMATE BODY CHARACTERISTICS (DIMENSIONS, DEPTHS AND DENSITY CONTRASTS) OF THREE DIMENSIONAL PRISMATIC BODIES BY APPLYING DIFFERENTIAL OPERATORS (GRADIENT ∇g , LAPLACIAN $\nabla^2 Z$ AND BIHARMONIC $\nabla^4 Z$) TO THEIR GRAVITY FIELDS.



Ali M. Al-Rahim

University of Baghdad - College of Science.

ARTICLE INFO

Received: 8 / 10 /2010
Accepted: 10 / 3 /2012
Available online: 14/6/2012
DOI: [10.37652/juaps.2011.44071](https://doi.org/10.37652/juaps.2011.44071)

Keywords:

Gravity,
Depth Estimation,
Prismatic bodies,
Differential Operator,
Gradient,
Laplacian,
Biharmonic.

ABSTRACT

Differential Operators (Gradient, Laplacian and Biharmonic) have been used to determine anomaly characteristics using theoretical gravity field for prismatic bodies with different top depths, dimensions and density contrasts. The concepts of gradient and laplacian operator are widely used in image processing. The intersection between the gravity field and the three differential operator's fields could be used to estimate the depth to the top of the prismatic bodies regardless of their differences in dimensions, depths and density contrasts. The Biharmonic Operator has an excellent result, were two zero closed contour line produced. The outline of the internal closed zero contour line define precisely the dimension of the prismatic bodies. The distance between this zero contour and the maxima of the Laplacian Operator define the exact depth to the top of the prismatic bodies. The maxima of the Biharmonic amplitude could be used for density contrast approximation. This is the first attempt to use such technique for estimating body characteristics. Also, the Biharmonic Operator has high sensitivity to resolve hidden small anomaly due the effect of large neighborhood anomaly, the 2nd derivative Laplacian Filter could reveal these small anomaly but the Biharmonic Operator could indicate the exact depth. The user for such technique should be very care to the accuracy of digitizing the data due to the high sensitivity of Biharmonic Operator. The validity of the method is tested using field example for salt dome in Gulf Coast basin.

Introduction:

Defining depth to the top or center of simple geometrical bodies using its gravity data is greatly help in interpretation of real field data. Several methods have been implemented for that from the beginning of using gravity in exploration geophysics at the 1930.

Due to the fast development in computer software that deal with mathematical approaches, new automated methods have been prepared and applied in

different studies. These methods tried to simplify the procedure as possible so that the interpreter could get the direct information for body characteristics directly from profiles or grid data.

The interpreter normally use simple geometrical shape models such as sphere, horizontal or vertical cylinder, dyke, prisms and contact (fault) and calculate their theoretical gravity effects to find any rules that could help him to know the depth directly from a profile measurements. For a spherical shape body, the half-width (X1/2) method is the commonest rules of thumb, these named Smith Rules (1). The maximum depth at

* Corresponding author at: University of Baghdad - College of Science. E-mail address: alial_rahim@yahoo.com

which the top of any particular geological body can be situated is known as the limiting depth. Methods of obtaining this information depend on which interpretational technique and model are being used (2). Another major important is to delineate the edge of the buried objects. The detection of border of subsurface bodies can be investigated by using either derivative based classical approaches or contemporary image processing algorithms (3).

Several numerical methods have been developed by various authors for interpreting gravity anomalies caused by simple models to find the depth of most geological structures. Excellent reviews are given by (4, 5). Nabighian et al. (5) presented excellent historical reviews for the development of the gravity method in exploration. Their paper included the main progress in gravity instrumentation, data reduction and processing, data filtering, enhancement and data interpretation. Also, they summarized a timeline of gravity exploration including the date and important event type.

For the first time, it has been proven by (6) that the Differential Operator could be used for delineating the depth to the center of spherical bodies using grid data and applied it for Salt Dome.

Prismatic bodies are widely used as an example for the purpose of defining depth. The present study is aiming to apply the Differential Operators (Gradient ∇g , Laplacian $\nabla^2 Z$ and Biharmonic $\nabla^4 Z$) on the theoretical gravity field of prismatic bodies and introducing a new novel method to get its edge boundary, density contrast and the depth to its top. This attempt is the first of using such technique in gravity interpretation for prismatic bodies.

The validity of the method is tested on field example for Salt Diapirs in Gulf Coast basin from an offshore area.

THEORETICAL BACK GROUND

The branch of mathematics that deals with derivatives is called Differential Calculus (7). Famous

contouring program - Surfer Program (Version 7.0 and later) (8) can calculate the Differential Operator for a grid data. The Differential Operator includes Gradient Operator, Laplacian Operator, and Biharmonic Operator.

Gradient Operator: generates a grid of steepest slopes (i.e. the magnitude of the gradient) at any point on the surface (9). The Gradient Operator is zero for a horizontal surface, and approaches infinity as the slope approaches vertical. The definition of the gradient yields the following equation (8 and 9):

$$\nabla g = \sqrt{\left(\frac{\partial z}{\partial x}\right)^2 + \left(\frac{\partial z}{\partial y}\right)^2}$$

Laplacian Operator:

provides a measure of discharge or recharge on a surface (9). In grid files generated with the Laplacian Operator, recharge areas are positive, and discharge areas are negative. Groundwater, heat, and electrical charge are three examples of conservative physical quantities whose local flow rate is proportional to the local gradient. The Laplacian operator, $\nabla^2 Z$, is the mathematical tool that quantifies the net flow into (Laplacian > 0 , or areas of recharge) or out of (Laplacian < 0 , areas of discharge) a local control volume in such physical situations. The Laplacian Operator is defined in multivariable calculus by (8 and 9):

$$\nabla^2 Z = \frac{\partial^2 Z}{\partial x^2} + \frac{\partial^2 Z}{\partial y^2}$$

Grid filtering applies methods of digital image analysis to grids. The Laplacian Operator is equal to inverse second derivative operator by applying a simple 3x3 Laplacian filter which has the following coefficients:

0	-1	0
-1	4	-1
0	-1	0

on the original data using linear convolution

approach. (10) (This will be proven during the text).

In Image Processing the Laplacian responds to transitions in intensity, it is seldom used in practice for edge detection. As a second-order derivative, the Laplacian typically is unacceptably sensitive to noise (11).

Biharmonic Operator: Bending of thin plates and shells, viscous flow in porous media, and stress functions in linear elasticity are three examples of physical quantities that can be mathematically described Biharmonic Operator (13). The Biharmonic Operator $\nabla^4 Z$ is defined in multivariable calculus by (8 and 9):

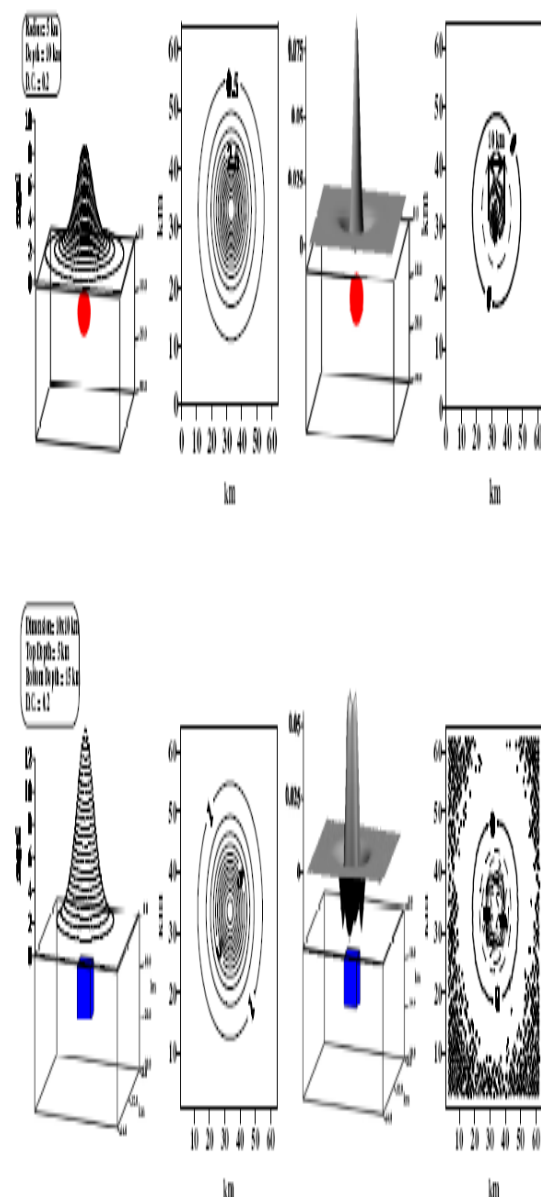
$$\nabla^4 Z = \frac{\partial^4 Z}{\partial x^4} + 2 \frac{\partial^4 Z}{\partial x^2 \partial y^2} + \frac{\partial^4 Z}{\partial y^4}$$

This is comparable to applying the Laplacian Operator twice (bilaplacian).

COMPARISON BETWEEN SPHERICAL AND PRISMATIC BODIES

Trying to develop the new novel method that has been presented by (6) for spherical bodies, a prism with dimension, depth and density contrast has been chosen to be with volume near to one of the spheres used by (6), the reason is to get a gravity field near in shape to the spherical body. So that, a prism with dimension 10x10 km, depth to the top of the prism is 5 km, depth to the bottom is 15 km and density contrast 0.2 g/cc (For prismatic bodies, a program designed by (13) has been used to calculate the gravity field of the prism). This prism has volume near to sphere with 5 km radius, 10 km depth to the center and 0.2 for density contrast. Figure (1) represents the 2D and 3D gravity field for both the sphere and prism. From the first looking to the figure, it is very difficult even for expert interpreter to resolve which one is related to sphere or prism (except the amplitude of the anomaly). But when applying the Biharmonic Operator for both models, it is clear that both of them are differs in shape. For spherical body,

the shape is like Mexican hat shape and the diameter of the zero closed interior contour determine directly the depth to the center of the spherical body (6). For the prismatic body the shape of the Biharmonic Operator has four protrusions and the zero closed contour has square shape with dimension exactly 10x10 km. This encourages the researcher to operate for more prismatic bodies to come across new ways for depth estimation for prismatic bodies.



The gravity field Its Biharmonic Operator
Fig. 1. 2D and 3D presentations for the gravity field of spherical and prismatic bodies and its Biharmonic Operator shapes. The spherical body has 5 km radius, 10 km depth to the center and 0.2 g/cc density contrast, while

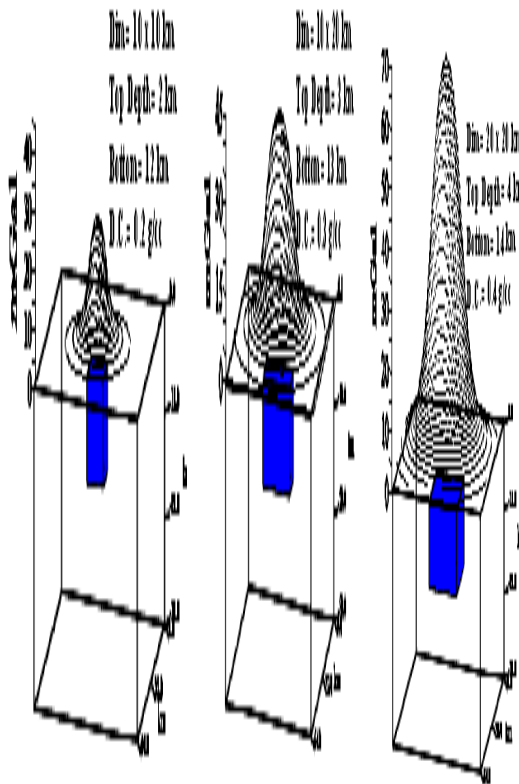
the prism has 10x10 km dimension, 5 km depth to the top, 15 km depth to the bottom and 0.2 g/cc density contrast.

METHODOLOGY

To apply the Differential Operator on the gravity field for simple prismatic shape, Program (13 using formula derived by 14) has been used for nine prisms with different dimensions, depths and density contrasts. For each prism, the theoretical gravity field has been calculated for three different density contrasts (0.2, 0.3 and 0.4 g/cc). The total cases used are 27. The dimension of the models is 64 x 64 km. Figures (2) illustrates 3D presentations for three of the 27 case mentioned above and table (1) shows the data used for each prism.

Table (1) shows the 27 cases used to apply by Differential Operator.

Prism No.1	Prism No.2	Prism No.3
Dimension: 10x10 km Top Depth: 2 km Bottom Depth: 12 km Density Contrast: 0.2, 0.3 and 0.4 g/cc.	Dimension: 10x10 km Top Depth: 3 km Bottom Depth: 13 km Density Contrast: 0.2, 0.3 and 0.4 g/cc.	Dimension: 10x10 km Top Depth: 4 km Bottom Depth: 14 km Density Contrast: 0.2, 0.3 and 0.4 g/cc.
Prism No.4	Prism No.5	Prism No.6
Dimension: 10x20 km Top Depth: 2 km Bottom Depth: 12 km Density Contrast: 0.2, 0.3 and 0.4 g/cc	Dimension: 10x20 km Top Depth: 3 km Bottom Depth: 13 km Density Contrast: 0.2, 0.3 and 0.4 g/cc	Dimension: 10x20 km Top Depth: 4 km Bottom Depth: 14 km Density Contrast: 0.2, 0.3 and 0.4 g/cc
Prism No.7	Prism No.8	Prism No.9
Dimension: 20x20 km Top Depth: 2 km Bottom Depth: 12 km Density Contrast: 0.2, 0.3 and 0.4 g/cc	Dimension: 20x20 km Top Depth: 3 km Bottom Depth: 13 km Density Contrast: 0.2, 0.3 and 0.4 g/cc	Dimension: 20x20 km Top Depth: 4 km Bottom Depth: 14 km Density Contrast: 0.2, 0.3 and 0.4 g/cc



(a) (b) (c)
Fig. 2. 3D Representation for the gravity field of prisms:

- (a) Dimension: 10x10 km, Top Depth: 2 km, Bottom Depth: 12 km, D.C.: 0.2 g/cc.
- (b) Dimension: 10x20 km, Top Depth: 3 km, Bottom Depth: 13 km, D.C.: 0.3 g/cc.
- (c) Dimension: 20x20 km, Top Depth: 4 km, Bottom Depth: 14 km, D.C.: 0.4 g/cc.

After that, Surfer version 9.0 program used to applying calculus – Differential Operator for all these 27 case. Figure (3) illustrates 2D and 3D representations for prism No.1 with dimension 10x10 km, depth to the top is 2 km and 12 km depth to the bottom with density contrast 0.2 g/cc. A slice profiles across the center of the four maps (Gravity, Gradient, Laplacian and Biharmonic) are plotted on one graph to be apple to compare between them as shown in figure (4). It is clear from figure (4) that the intersection between the gravity field and the three differential operator's fields could be used to estimate the width of the model and depth to the top of the prismatic body. Searching for the zero location of the Biharmonic curve is the start point of interpretation. The zero location comes exactly with the maxima of the Gradient where this place is perfect to define the contact location. The distance between the

two zero locations on the Biharmonic curve determine the width of the prism. The distance between the zeros on the internal part of the Biharmonic curve and the maxima on the Laplacian curve defines the depth to the top of the model. The amplitude of the Biharmonic maxima works as an indication key for density contrast (see later). The same approaches have been done for all prismatic models and give the same result regardless of their differences in dimensions, depths and density contracts. Figure (5 and 6) show examples of prisms with dimensions 10x20 and 20x20 km, top depths are 3 and 4 km with density contrasts 0.3 and 0.4 g/cc respectively.

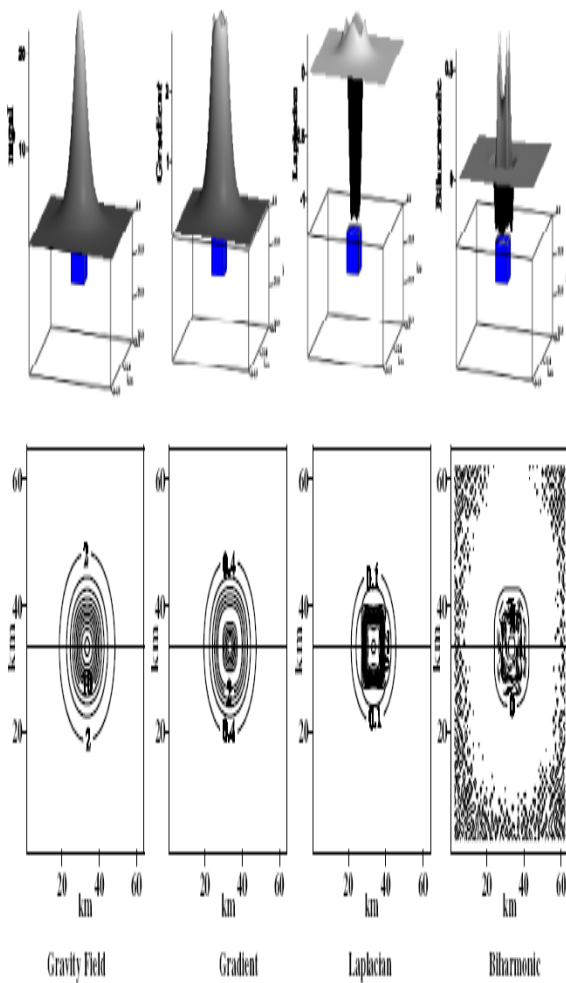


Fig. 3. 3D and 2D representations for prismatic case with dimension 10x10 km, top depth 2 km, bottom depth 12 km, and density contrast 0.2 g/cc. A profile taken across the middle part of each map (Gravity, Gradient, Laplacian and Biharmonic) and the result shown in Fig. 4.

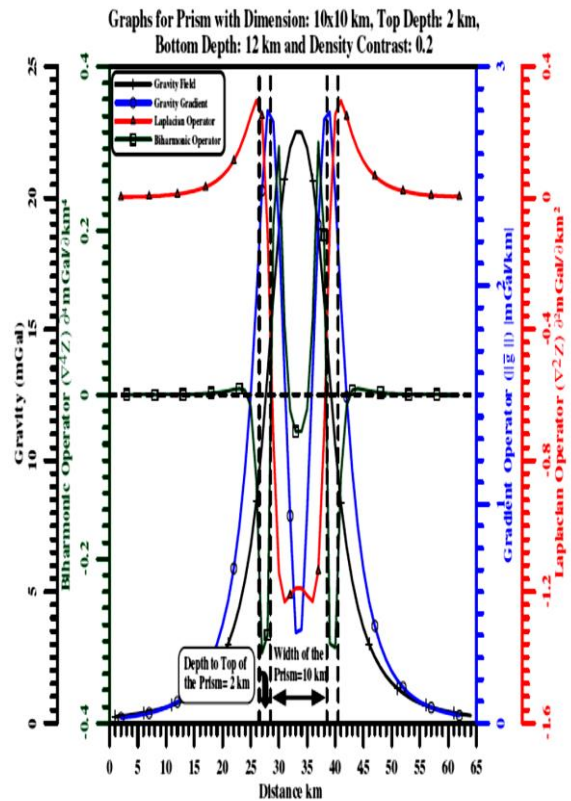


Fig. 4. Represents the profiles taken across the center of prisms maps shown in Fig. 3.

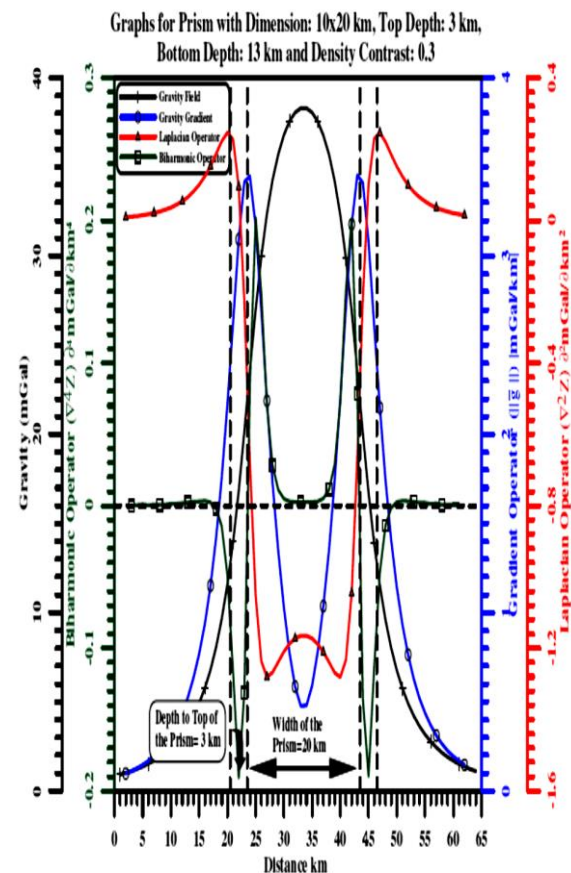


Fig. 5. Represents the profiles taken across the center of prism with dimension 10x20 km, top depth 3 km, bottom depth 13 km and density contrasts 0.3 g/cc.

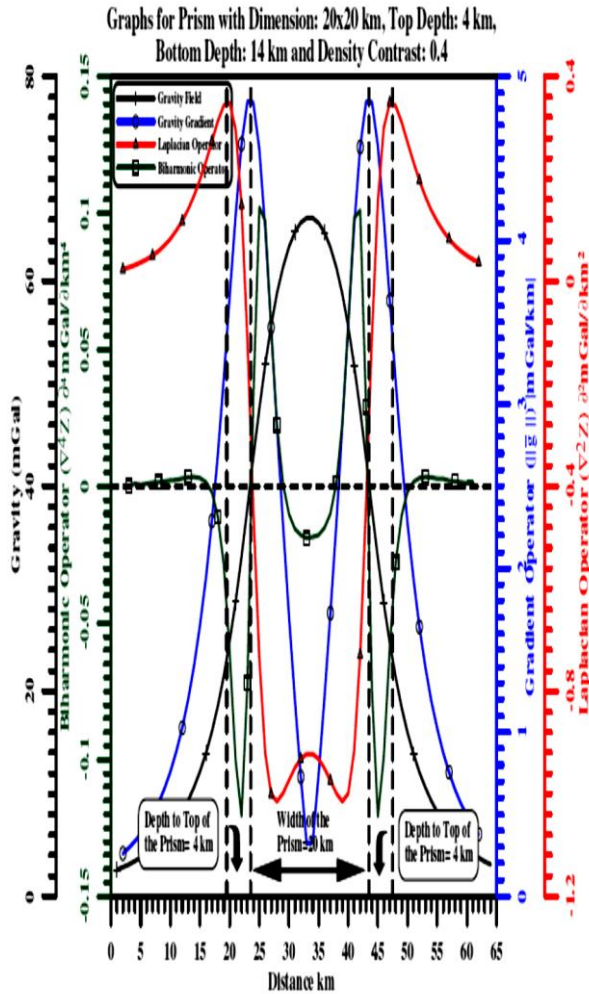
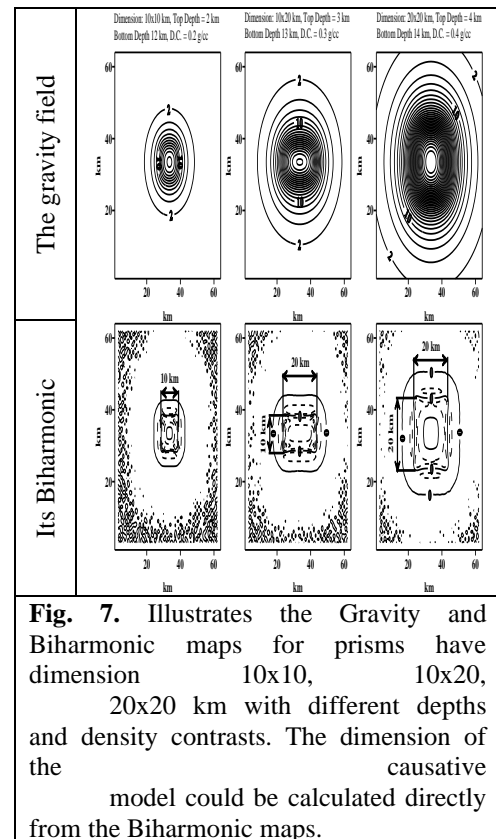


Fig. 6. Represents the profiles taken across the center of prism with dimension 20x20 km, top depth 4 km, bottom depth 14 km and density contrasts 0.4 g/cc.

Return back to figure (3), its clear that the Biharmonic Operator map has two zero closed contours. The internal one circumscribes four protrusions (one for each corner of the prismatic model) and has square shape with dimension exactly 10x10 km. This dimension of the internal zero contour defines the exact location of the prism. This characteristic of the internal zero contour of the Biharmonic Operator map has an excellent denote to define the boundary of the models and the exact dimension could be measured directly. Figure (7) is an example of such process for different prisms.

Another remark is that the Biharmonic map has a protrusion along each corner of the anomaly. If the anomalies body has no corner such as sphere, the

Biharmonic map will has Mexican hat shape (6), See figure (1).



Density Contrast

To find the relation between the Biharmonic Operator map and density contrast with depth, a bar chart diagram is plotted in figure (8) for the 27 cases used in test. The maximum amplitude of the protrusion in the Biharmonic map is plotted against density contrast and depth. It is clear from the chart that the Biharmonic amplitude has the same shape for prisms with dimension 10x10, 10x20 and 20x20 km. That is mean; the dimension of the prism has no effect. The difference in depth dramatically affect on the Biharmonic amplitude. Figure (8) can be used to define the density contrast if the depth to the top of the model is known in the way described above. For depth to the top 4 km; the amplitude of the Biharmonic map never exceed 0.2; for 3 km top depth it is between 0.2-0.6 and for 2 km top depth it is more than 0.6.

Applying this procedure to our first tested prism (compared to sphere shown in figure 1), figure (9) present the result for the depth of the prism.

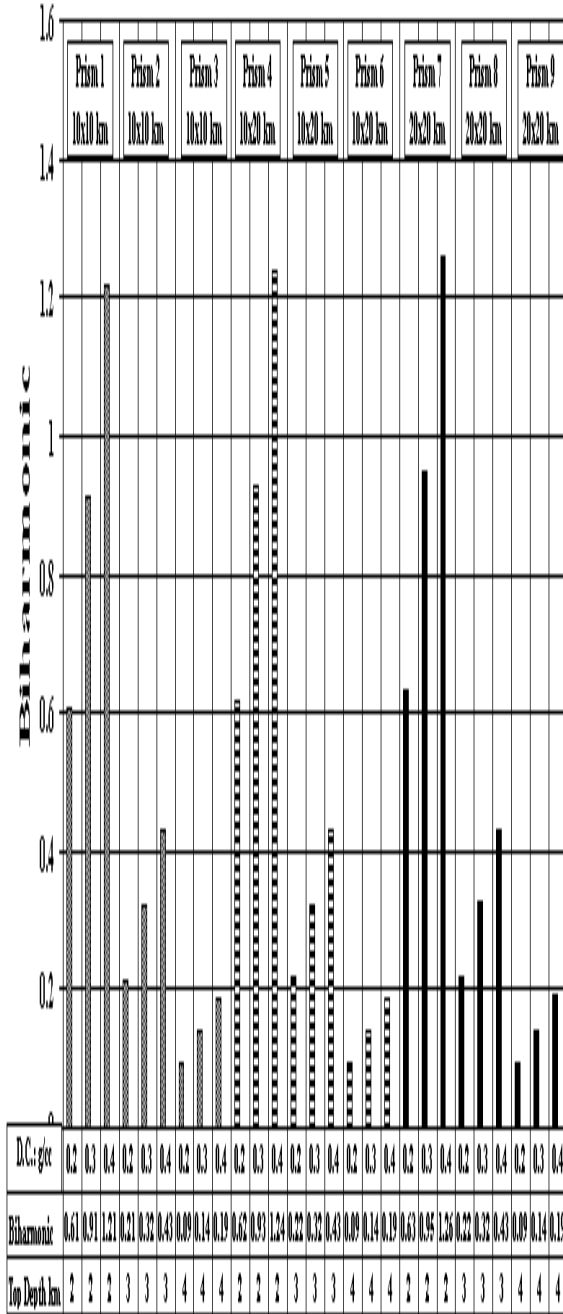


Fig. 8. A bar chart diagram is plotted for the 27 cases used in test. The maximum amplitude of the protrusion in the Biharmonic map is plotted against density contrast and depth. It is clear from the chart that the Biharmonic amplitude has the same shape for prisms with dimension 10x10, 10x20 and 20x20 km. That is mean; the dimension of the prism has no effect.

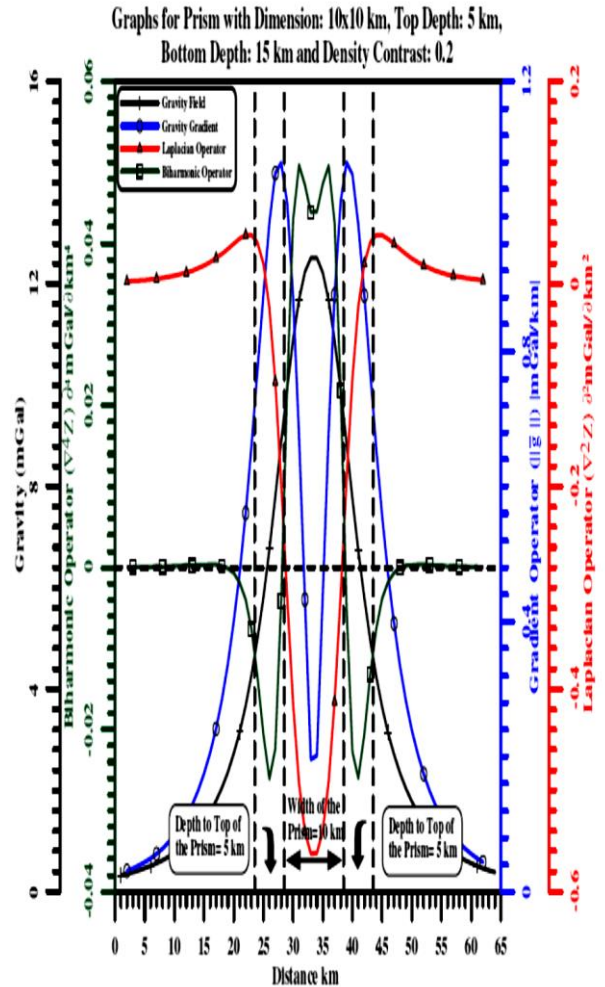


Fig. 9. Represents the profiles taken across the center of compared prism in Fig.(1) with dimension 10x10 km, top depth 5 km, bottom depth 15 km and density contrast 0.2g/cc.

COMPLICATING THE TEST

Trying to test the procedure on complicated models, a case for two contact prisms with different dimensions (10x10 km and 10x20 km), but have the same top depth (2 km) and density contrast (0.2 g/cc). Figure (10) shows 2D and 3D representations for this model. The Biharmonic 2D and 3D give perfect boundary dimension of the two prisms. Six protrusions define the six corner of the model where it esteemed as one body. Three profiles are taken across the model to estimate the depth. Two are taken across each prism and the third is taken vertically on both of them (See Fig. 10). Figure (11) illustrates these profiles and the procedure for estimate depth is correctly specified.

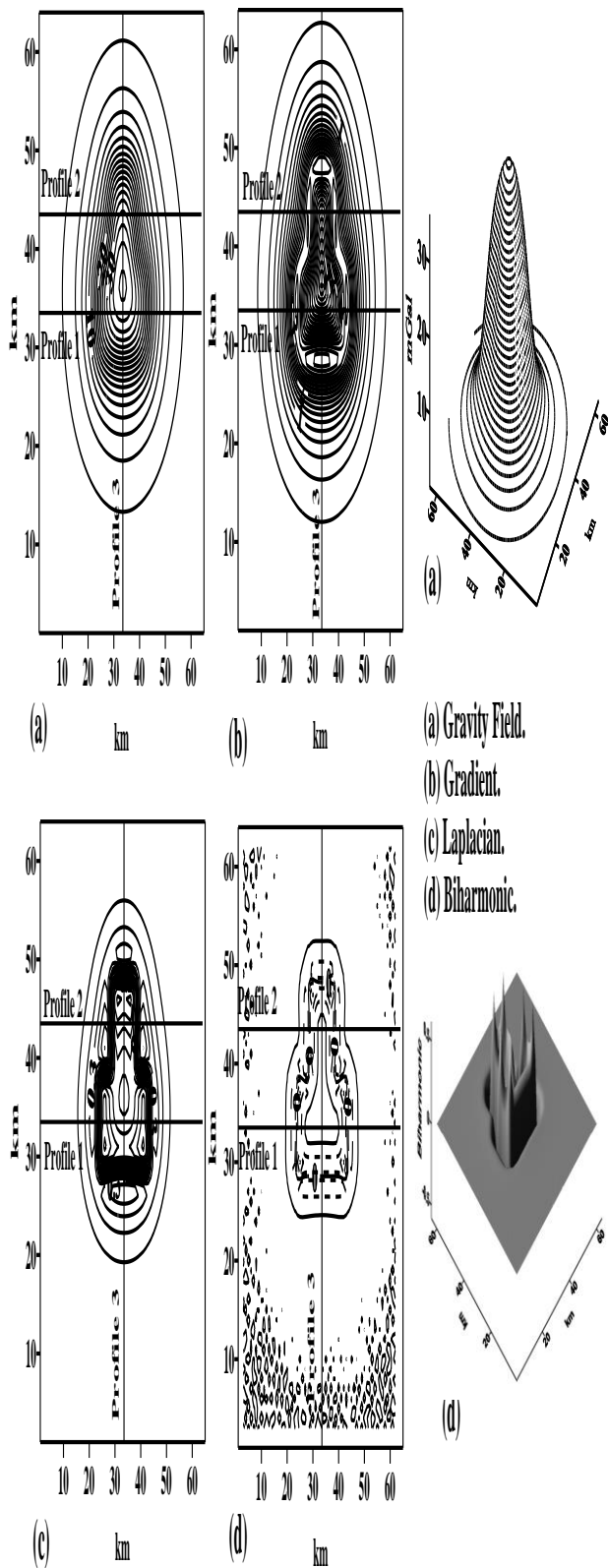


Fig. 10. Shows 2D and 3D representations of a complicated model. A case for two contact prisms with different dimensions (10x10 km and 10x20 km), but have the same top depth (2 km) and density contrast (0.2 g/cc).

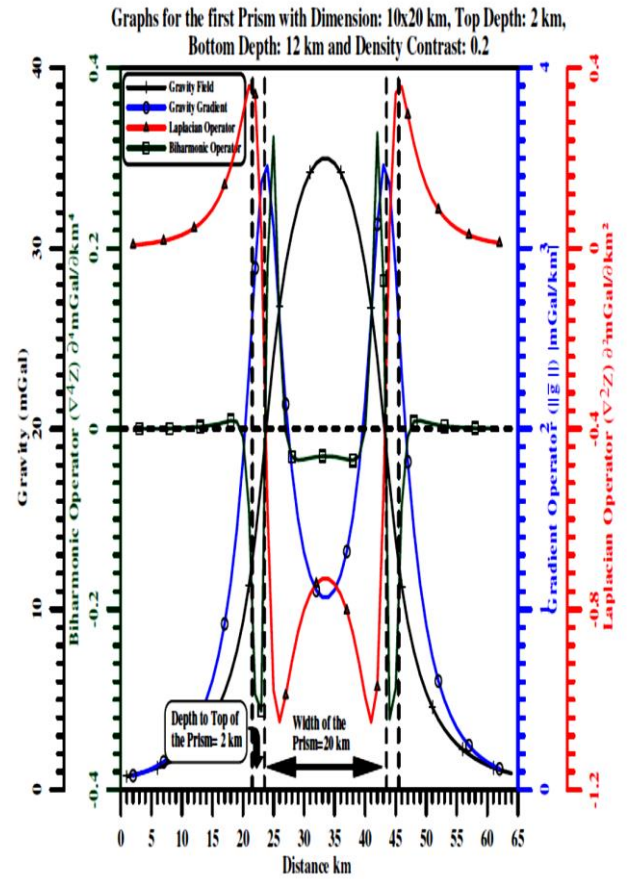


Fig. 11. a) Profile 1

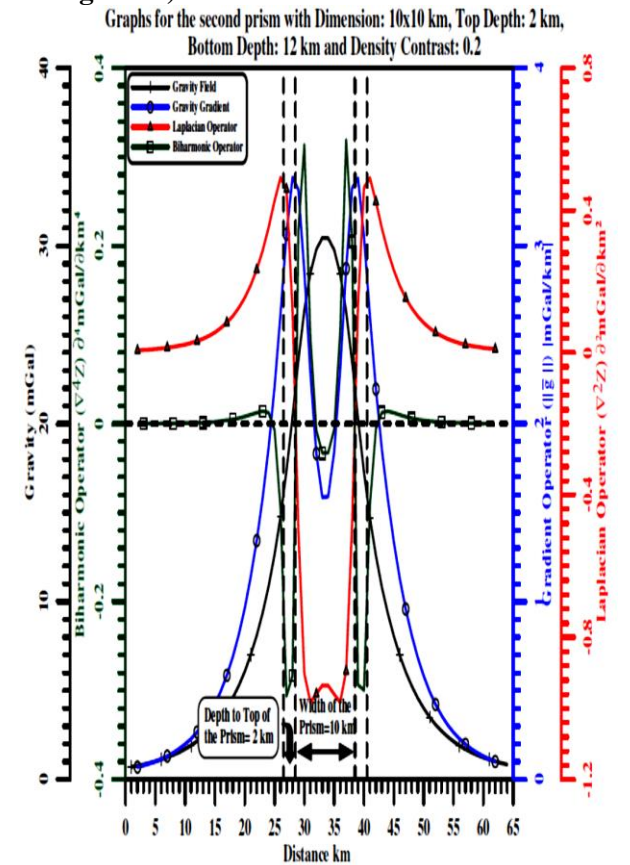


Fig. 11. b) Profile 2

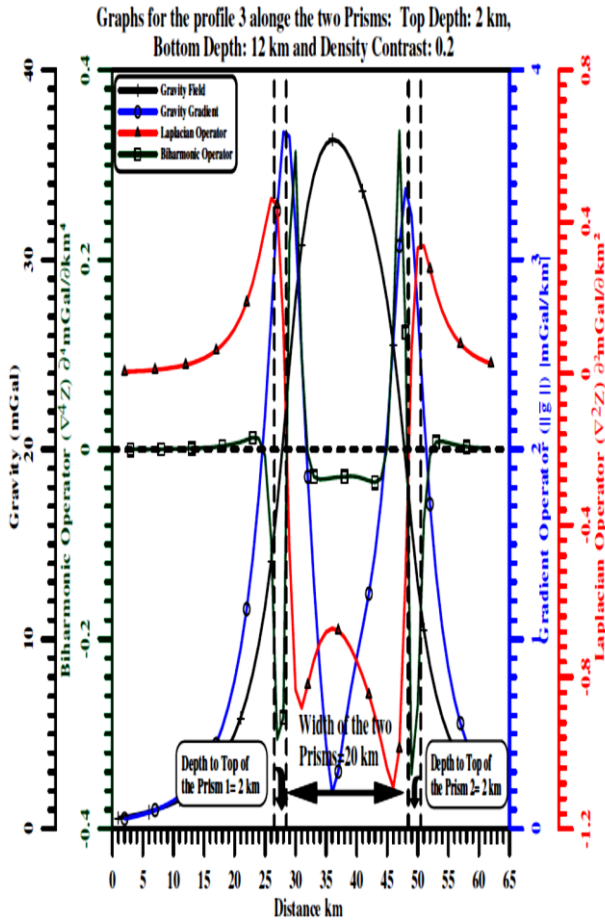


Fig. 11. c) Profile 3

Fig. 11. (a, b and c) Illustrates three profiles taken across two prisms shown in figure (10). The procedure for estimating depth is correctly specified for this model.

Second example has been taken using two prisms with (10x10 km and 10x20 km dimension, density contrast 0.2 g/cc but with different depths to the top (2 km and 4 km). Figure (12) illustrates 2D and 3D representations of the calculated gravity and its Differential Operator. The Biharmonic map (2D and 3D) is clearly defining the difference in amplitude due to its difference in depth. The horizontal profiles (1 and 2) have no problem in depth estimation, see figure (13). While with profile 3, the depth should be estimated from outside part of the profile. The contact between the two prisms could be defined directly from the zero point of the Biharmonic profile in its middle part. Attracting attention is for the difference in the amplitude of the Biharmonic values.

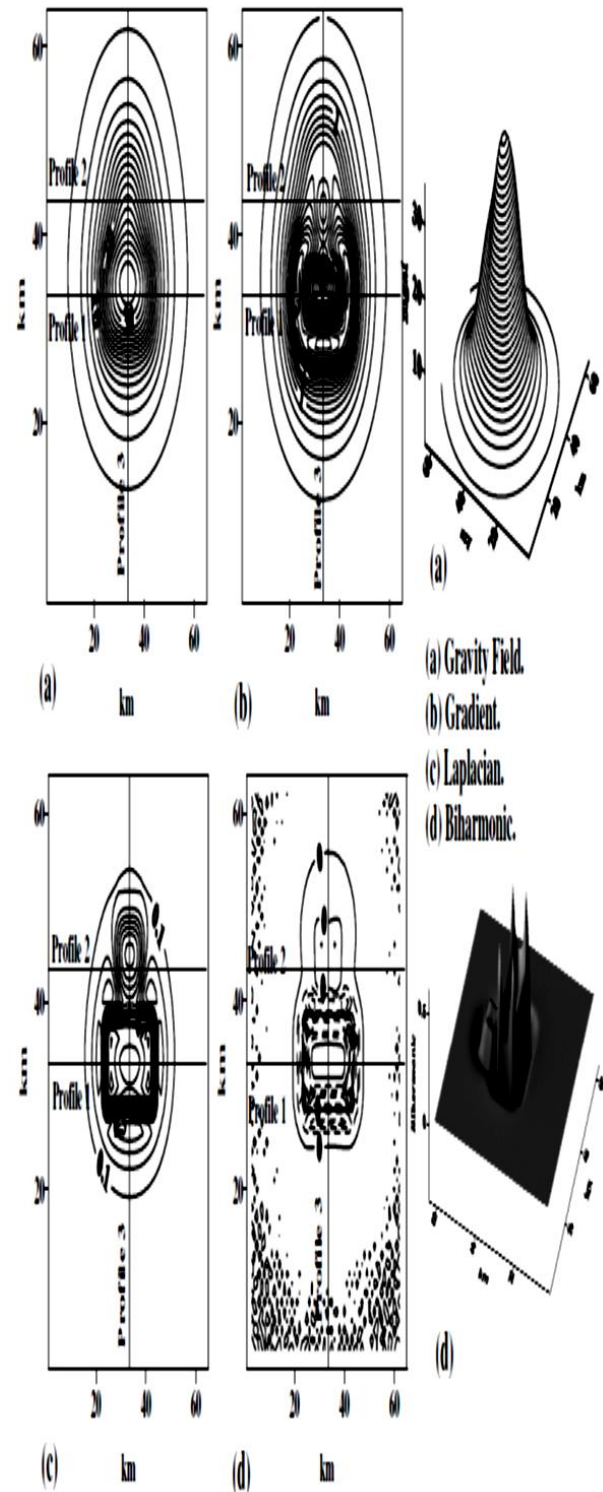


Fig. 12. Shows 2D and 3D representations of the second complicated model. A case for two contact prisms with different dimensions (10x10 km and 10x20 km), density contrast (0.2g/cc) but with different depths to the top (2 km and 4km).

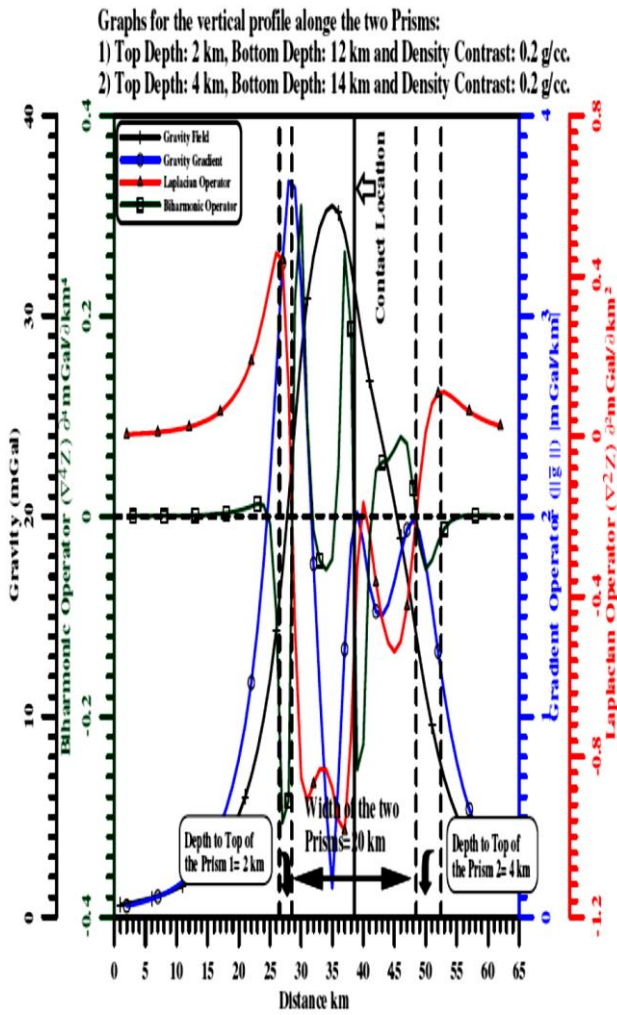


Fig. 13. Profile 3 of the second example (Figure 12), the depth should be estimated from outside part of the profile. The contact between the two prisms could be defined directly from the zero point of the Biharmonic profile in its middle part. Attracting attention is for the difference in the amplitude of the Biharmonic values.

Third example has been taken using two prisms with (10x10 km and 10x20 km dimension, 2 km depth to the top of the two prisms but with different density contrasts 0.2 g/cc and 0.4 g/cc. Figure (14) illustrate 2D and 3D representations of the calculated gravity and it's Differential Operator. The Biharmonic maps (2D and 3D) are clearly have less difference in amplitude due its same depth but the difference is in density contrast. Again, the horizontal profiles (1 and 2) have no problem in depth estimation, see figure (15). While with profile 3, the depth should be estimated from outside part of the profile. The contact between the two prisms could be defined directly from the zero point of the Biharmonic profile in its middle part.

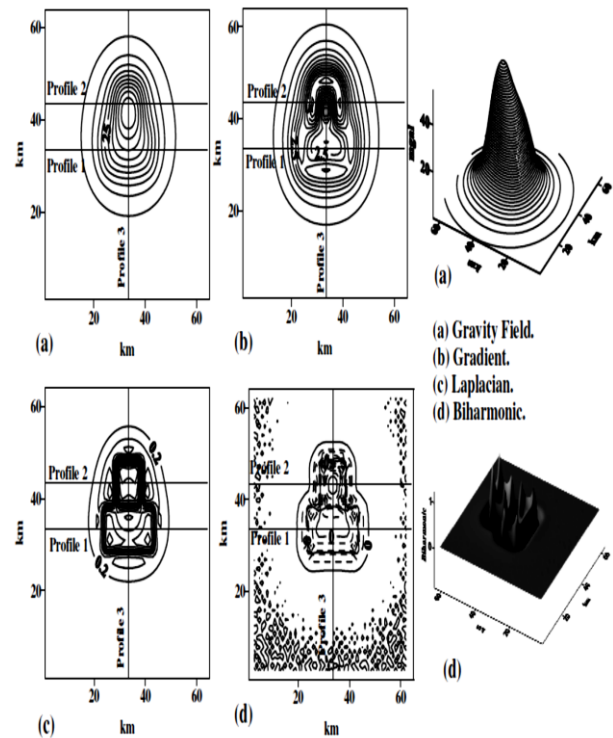


Fig. 14. Shows 2D and 3D representations of the third complicated model. A case for two contact prisms with different dimensions (10x10 km and 10x20 km), depth to the top (2 km), but with different density contrasts (0.2 and 0.4) g/cc.

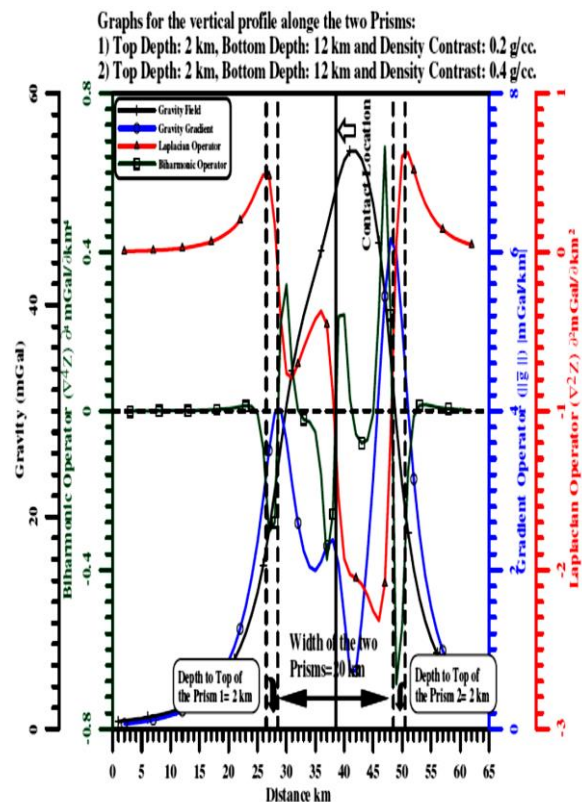


Fig. 15. Profile 3 of the third example (Figure 14), the depth should be estimated from outside part of the profile. The contact between the two prisms could be defined directly from the zero point of the Biharmonic profile in its middle part.

SMALL TARGET

In potential fields' survey, the observed data comprise the sum of the effects produced by all underground sources. The targets are often small-scale structures buried at shallow or deep depths. The response of these targets is superimposed in a regional field or other targets which arises from underground or neighboring sources that are usually larger in size and/or buried deeper. Trying to test the procedure on more complicated models, a case for three prisms with different dimension, top depth, and density contrast are taken as follow:

Prism 1	Dimension: 10x20 km Depth to top: 2 km Depth to bottom:12 km Density Contrast:0.3 g/cc
Prism 2	Dimension: 10x10 km Depth to top: 4 km Depth to bottom:14 km Density Contrast:0.2 g/cc
Prism 3	Dimension: 10x20 km Depth to top: 2 km Depth to bottom:12 km Density Contrast:0.4 g/cc

Figure (16) shows 2D and 3D representations for this model. From the gravity map in figure (16, a), it's very difficult to recognize the small prism in the middle part due to the effect of surrounding two prisms that have larger size and density contrast. This is a case where juxtapose small body cannot be clearly distinguished on the basis of anomaly data.

The 3x3 second derivative Laplacian filter with coefficient mentioned at the theoretical back ground could resolve these anomalies. The Laplacian filter produces a curvature map in which inflection points in the original data are located at the zero contours Figure (17). These procedures are widely used in image processing technique. (As mentioned in the theoretical back ground, that the Laplacian Operator is equal to inverse second derivative operator (figure (17)) prove this remark). But, the Biharmonic Operator could also resolve the anomaly for prism no. 2 and determine its boundary accurately. With no doubt, its depth

calculation will be less accurate due to the effect of direct contact of prisms 1 and 2. Also, the depth for prism 1 and 2 should be calculated from the outer part of the anomalies to reduce its effect.

Seeing figure (18) for profile 3 graphs, it is clear that the gravity profile could not be able to resolve the middle prism due to its smallest size, deeper depth and lowest density contrast, in spite of that the Differential Operator plays a new important rule for estimating depth, boundary location and density contrast.

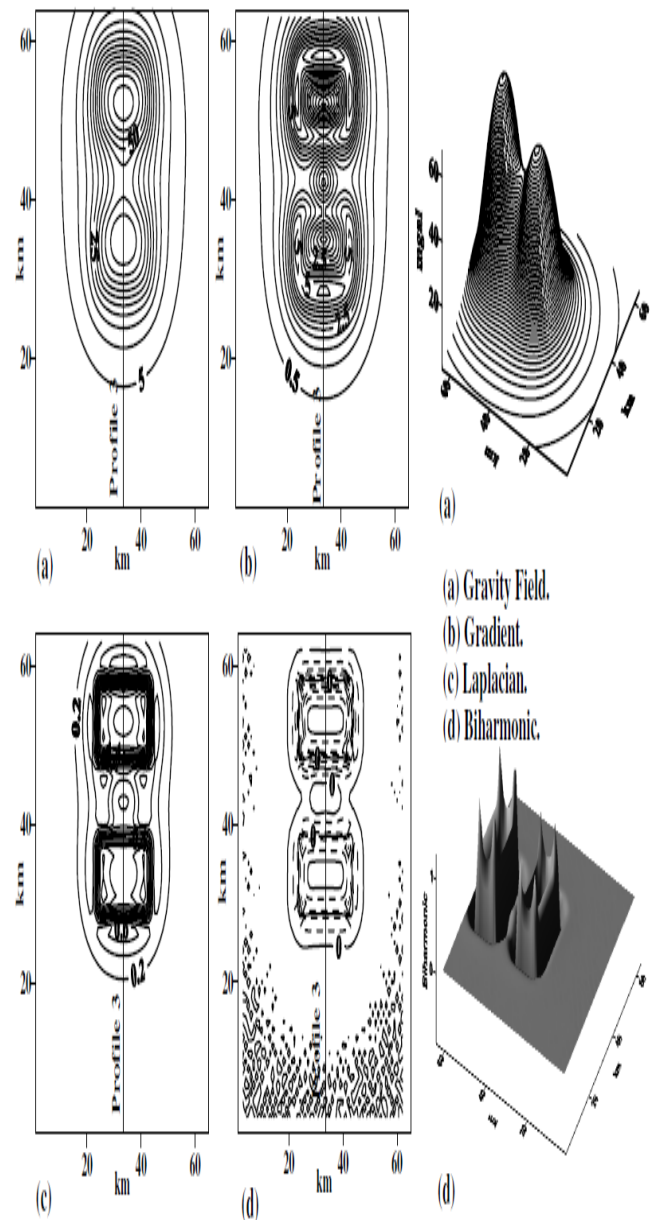


Fig. 16. Shows 2D and 3D representations of the small target case. The parameters of the model are mentioned in the text of the paper.

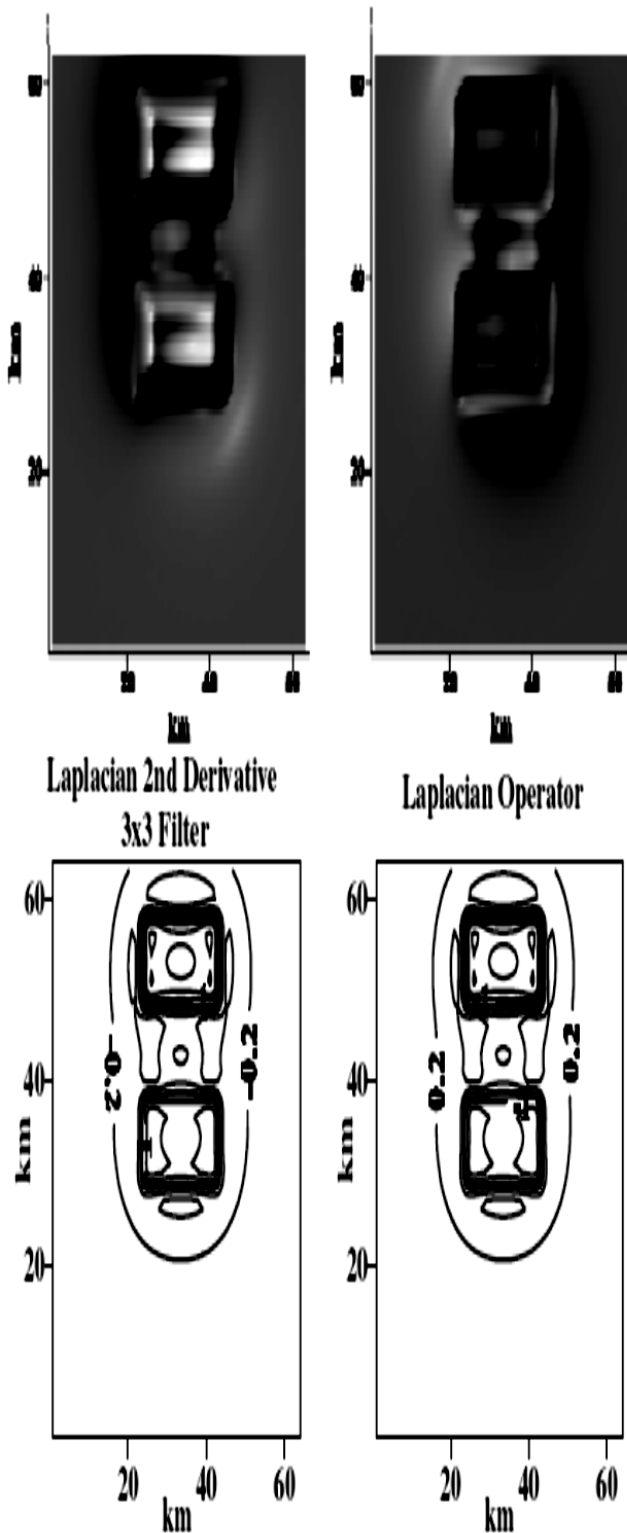


Fig. 17. 2D and 3D representations of the Laplacian 2nd Derivative 3x3 Filter which is the inverse of the Laplacian Differential Operator.

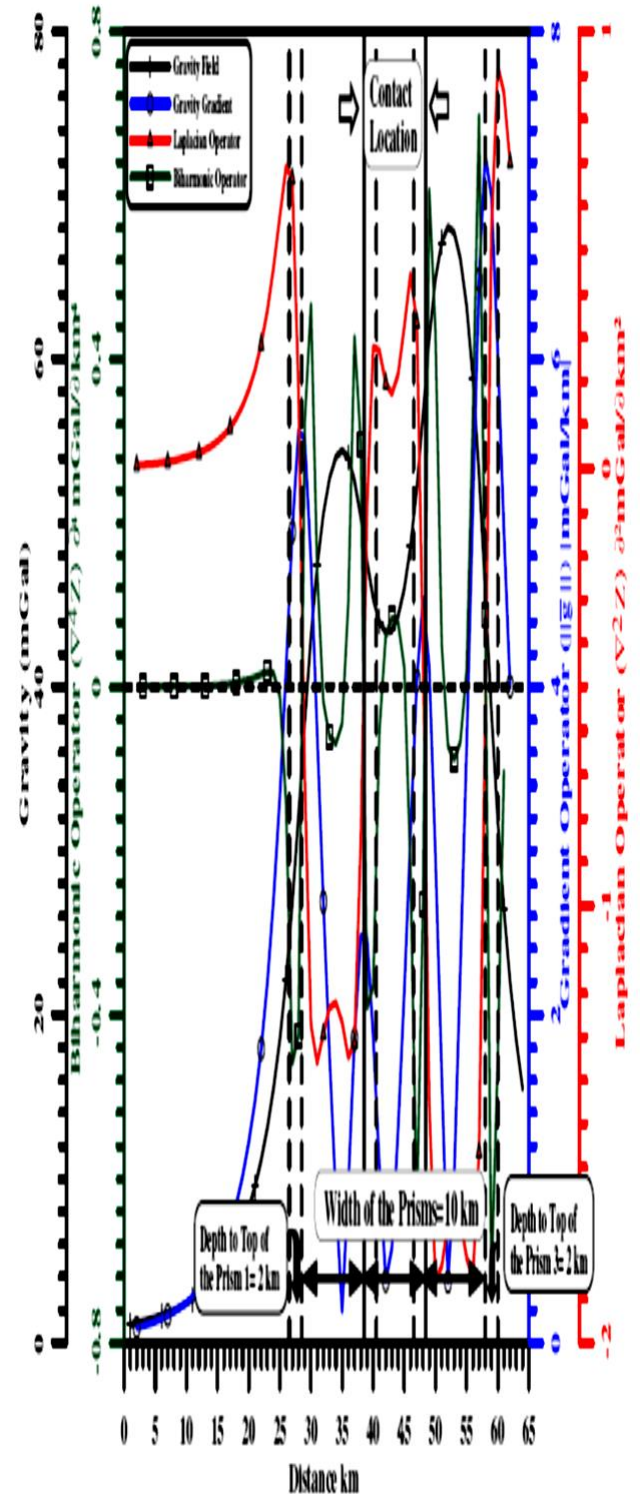


Fig. 18. Graphs for profile 3 along the three prisms shown in figure (16):

- 1) Dimension: 10x20km, Top Depth: 2 km, Bottom Depth: 12 km and D.C.: 0.3 g/cc.
- 2) Dimension: 10x10km, Top Depth: 4 km, Bottom Depth: 14 km and D.C.: 0.2 g/cc.
- 3) Dimension: 10x20km, Top Depth: 2 km, Bottom Depth: 12 km and D.C.: 0.4 g/cc. The gravity profile has no indication for the small middle target, while the Differential Operator graphs have better result.

FIELD EXAMPLE

It is very hard to find a typical example for three dimensional prismatic bodies; also, most authors avoid dealing with three dimensional cases. Most of them took a profile across the center of an anomaly and applied simplified interpretation tools to get reasonable results. These are due to difficulties in finding typical field example for prismatic body hypothesis. For that the field example is taken for Salt Diapir in the Gulf Coast basin area and interpreted using the assumption of vertical cylinder (15, page 221 Figure 3.40). The Bouguer gravity map of this example is given in Figure (19). The interpreter in (15) took a profile across the middle

part of the anomaly and used the assumption of vertical cylinder. The depth to the top is found to be 7.3 kft, radius is 3.85 kft and density contrast is -0.3 gm/cm^3 . The interpretation was not supported by any drilling test and this interpretation is only a hypothetical case to attempt some quantitative estimation even it has less confidence to the results (15). But, when looking to the residual map (Fig. 19 b) it is obvious that the anomaly has elongated shape and the assumption of prism interpretation is more suitable. Also, there is a low gradient in the upper part of the anomaly and suggested another small body, for that different type of analytical process has been applied to prove this assumption.

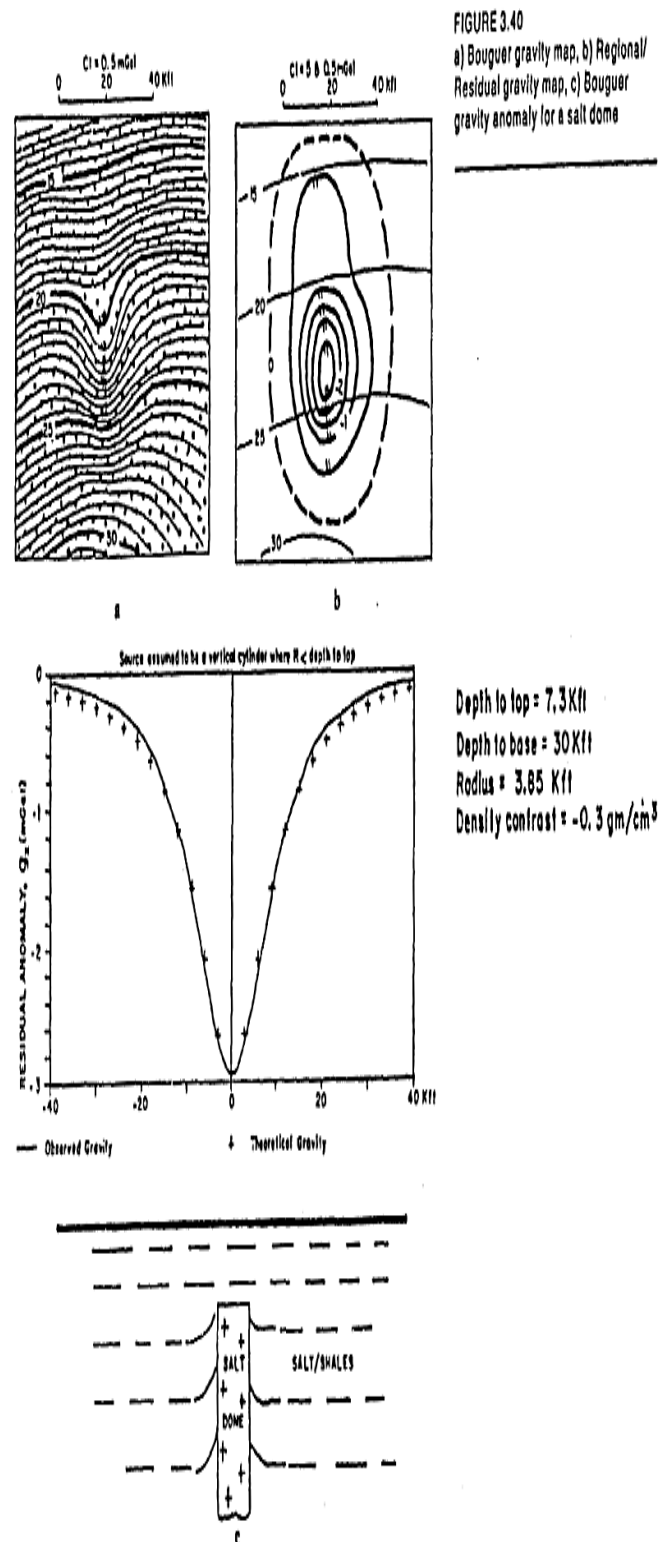


Fig. 19. Salt Diapir example anomaly is chosen as a field example (15, page 221 Figure 3.40). The interpreter in (15) takes a profile across the middle part of the anomaly and uses the assumption of vertical cylinder. The depth to the top is founded to be 7.3 kft, radius is 3.85 kft and density contrast is -0.3 gm/cm^3 (15).

The Differential Operators are very sensitive because they are dealing with derivatives of different degrees, where the high frequency signals will amplified greatly due to this

process. The different in data gradient also affects the result. White noise data form small error in digitization of the original data also amplified by derivatives of different degrees. All these facts must be taken in consideration and a type of smoothing should be applied to the data to enhance the signal-to-noise ratio. Many authors discussed these effects especially for method that use derivatives in depth estimation. Pašteka et al. (16) presented most up-to-date summery for this problem and suggested a type of regularized filter to damp the amplification of the high frequency content in the processed signal.

For that, smoothing the input data is mandatory to get reasonable result. Figure (20 a) gives a smooth digitized gravity field for the case study area. Figure (20 b, c and d) is the output of Gradient, Laplacian and Biharmonic Operators. The Gradient map clearly shows that the middle part of the anomaly has highest gradient with some elongation shape. But, another high gradient could be found easily in the northern part with east-west direction. The Laplacian Operator map gives the same result. Matrix smooth with 1x1 cell is applied to the Biharmonic map Figure (20 d). The zero closed contour line for the Biharmonic map shows the exact boundary of the diapirs body (Gray area in figure 20 d). The body clearly has elongated shape and the upper one with small size.

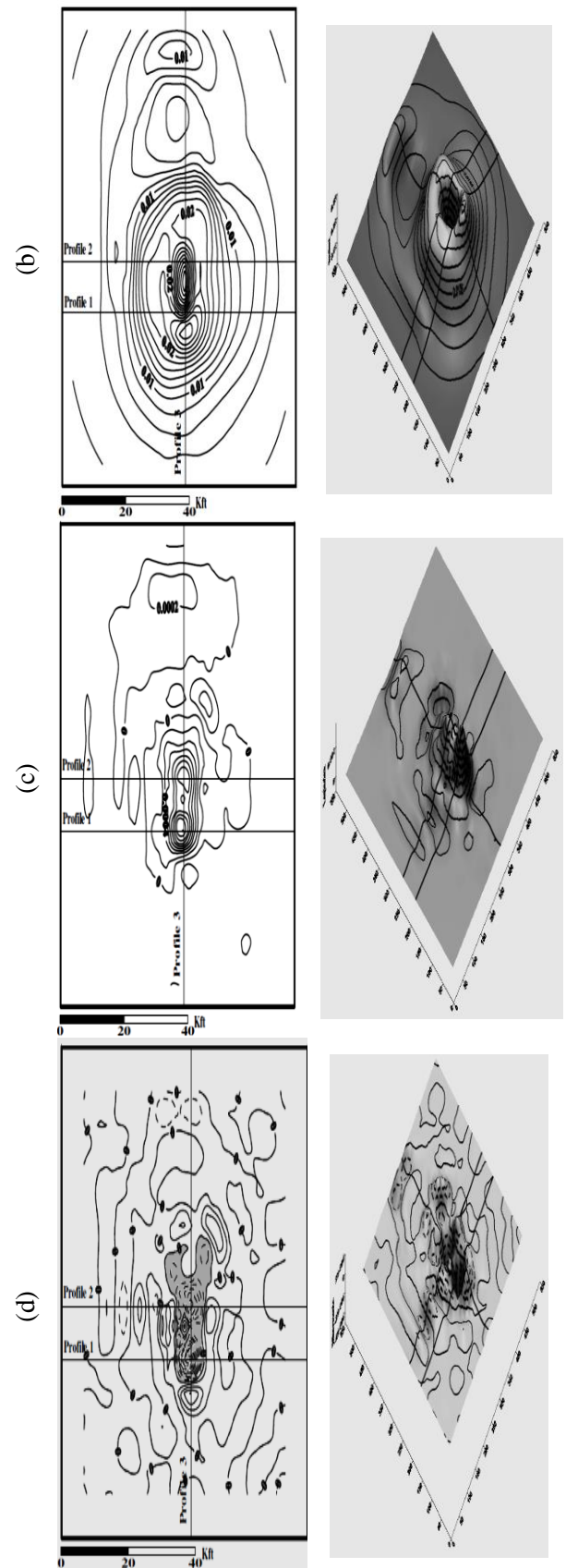
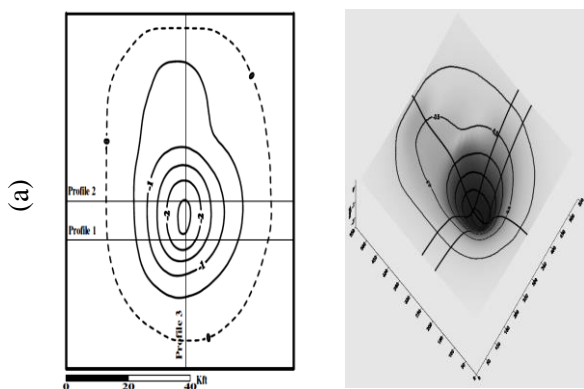


Fig. 20. a- 2D and 3D digitized map for the Bouguer gravity map of Salt Dome.
 b- 2D and 3D representation for the Gradient Operator.
 c- 2D and 3D representation for the Laplacian Operator.
 d- 2D and 3D representation for the Biharmonic Operator.
 The zero closed contour (Gray area) define the dimensions of salt dome, its boundary and directions.

Attempting to emphasize the upper small body, a difference of Gaussian (9x9) second derivative with the following coefficient (9):

0	0	0	-1	-1	-1	0	0	0
0	-2	-3	-3	-3	-3	-3	-2	0
0	-3	-2	-1	-1	-1	-2	-3	0
-1	-3	-1	9	9	9	-1	-3	-1
-1	-3	-1	9	19	9	-1	-3	-1
-1	-3	-1	9	9	9	-1	-3	-1
0	-3	-2	-1	-1	-1	-2	-3	0
0	-2	-3	-3	-3	-3	-3	-2	0
0	0	0	-1	-1	-1	0	0	0

has been applied to the anomaly map depending on the concept of convolution and the result shown in figure (21). The zero contour line determines the boundary of the anomaly. The light gray area within the closed zero contour defines the boundary of the causative body. The upper part has more realistic characterization.

Modeling profile figure (22) supports the assumption for the upper small body (See the vertical profile in figure 20a for comparison). The density contrast for prism used in the centered model is -0.2 g/cc while the small body has given -0.1 g/cc.

Figure (23) illustrates the direct calculation of the depth across two transversal profiles through the anomaly maxima and one vertical profile is taken across the middle part. The calculated depth differs from side to side.

The following table summarized the calculated depths:

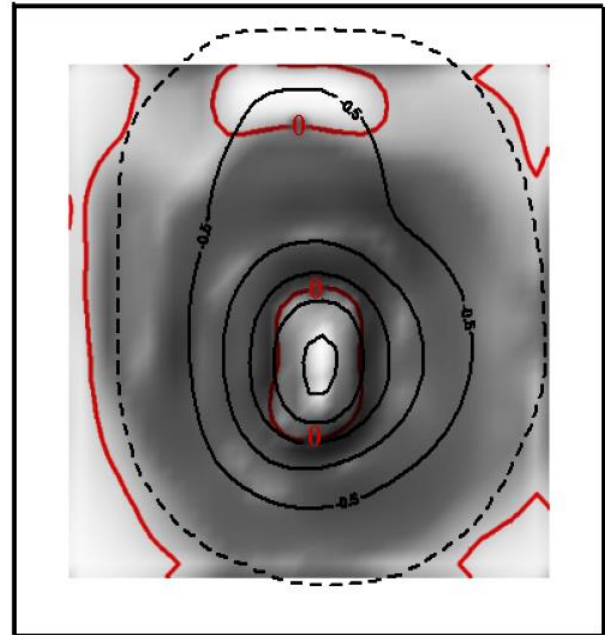


Fig. 21. Map of Difference of Gaussian second derivative with (9x9) coefficient superimposed by the example map. The light gray area within the closed zero contour define the boundary of the causative body.

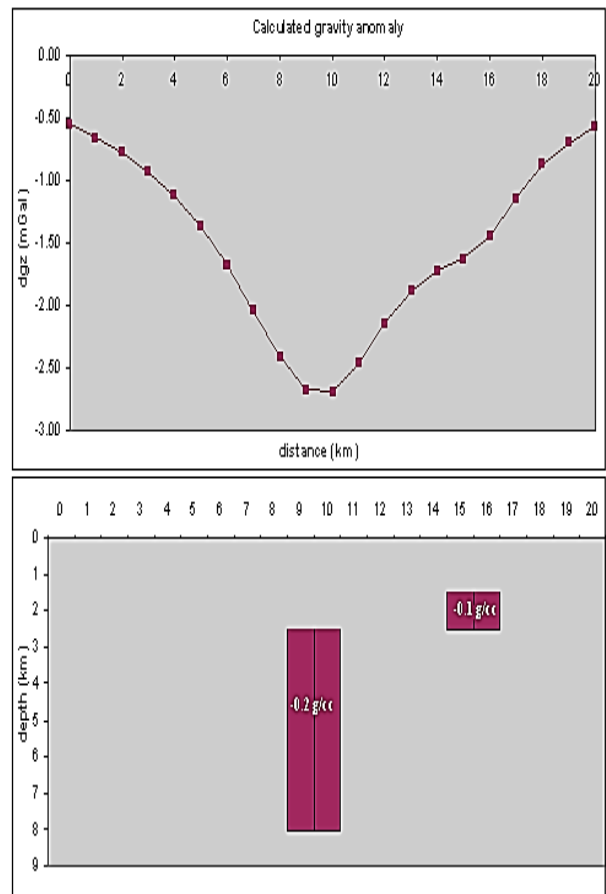


Fig. 22. Estimated modeling profile supports the assumption of the upper small body (See the vertical profile in figure 23a for comparison of the gravity profile).

Profile	Body	Left depth	Right
---------	------	------------	-------

No.	width		depth
1	8.32 kft	4.17 kft	5.46 kft
2	8.61 kft	5.61 kft	5.75 kft
3	15.95 kft	6.31 kft	-----
2nd body in profile 3	5.46 kft	-----	3.4 kft

For profile 3 the correct depth calculated from the left side of the central salt dome, the 2nd body depth is calculated from its right side. This is the suitable way for depth estimation as mentioned above in the complicate tested body.

The calculated depths are little differing from that presented by (15) due to the difference on the depended assumption. Also, defining the second body is new.

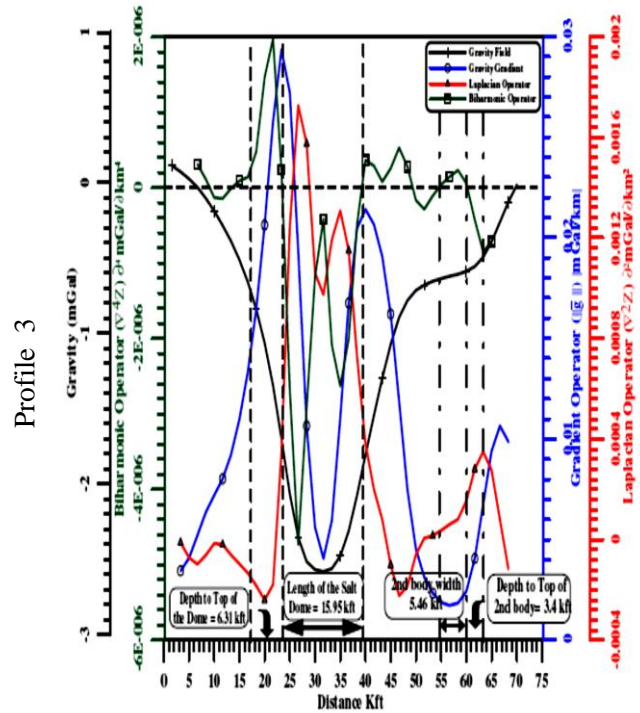
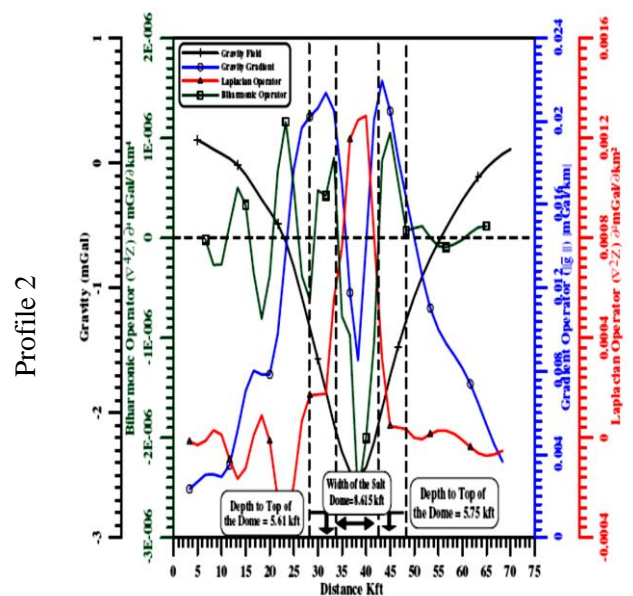
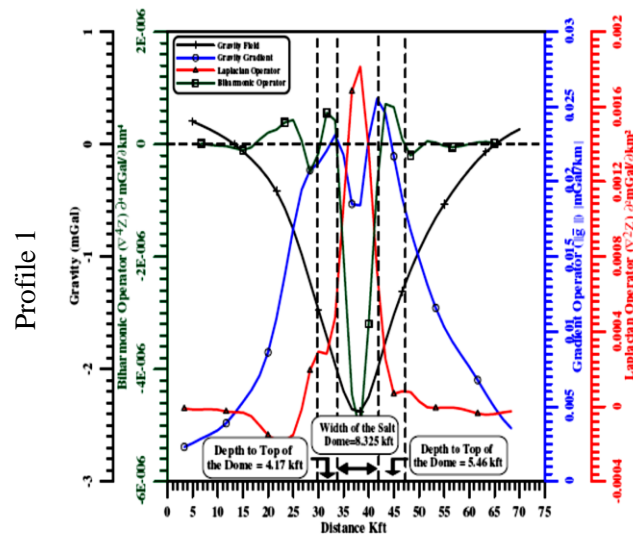


Fig. 23. Illustrates the direct depth estimation for profile 1, 2 and 3 for the field example case.

CONCLUSION

For the first time, the Differential Operators are operated to the gravity field of prismatic bodies to define their characteristic (top depths, dimensions and density contracts). The Biharmonic Operator is very sensitive to determine the shape and depth where the zero closed contour is the key factor for that, its amplitude could be used to determine the density contrast.

ACKNOWLEDGMENTS

The author would like to thank Dr. Amin Al-Yasi (Dep. of Earth Sciences –College of Science - University of Baghdad – IRAQ) for his excellent suggestion and reviewing the manuscript of this paper.

REFERENCES:

1- Smith, R.A. (1960). Some formulae for interpreting local gravity anomalies. Geophysical Prospecting, Vol. 8: No. 4: P 607-613.

- 2- Reynolds, J. M. (1998). An Introduction to Applied and Environmental Geophysics. John Wiley & Sons Ltd.
- 3- Ucan, O.N., Alhora, A.M. and Ozmen, A. (2003). Evaluation of tectonic structure of Gelibolu (Turkey) using steerable filters. J. of the Balkan Geophysical Society. Vol. 6: No. 4: P221-234.
- 4- El-Sayed, M. A. and El-Araby, T.M. (1993) A least-square minimization approach to depth determination from moving average residual gravity anomalies. Geophysics. Vol. 59: No. 12: P1779-1784.
- 5- Nabughian, M.N., Ander, M.E., Grauch, V.J.S., Hansen, R.O., LaFehr, T.R., Li, Y., Pearson, W.C., Peirce, J.W., Phillips, J.D., and Ruder, M.E. (2005). 75th Anniversary Historical development of the gravity method in exploration. Geophysics. Vol. 70: No. 6: P63ND-89ND.
- 6- Al-Rahim, A. M. (2009). Depth estimation of spherical bodies using Differential Operators (Gradient $\nabla \bar{g}$, Laplacian $\nabla^2 Z$ and Biharmonic $\nabla^4 Z$) to its gravity fields. J. of University of Anbar for Pure Science. Vol. 3: No. 3: P 74-85.
- 7- Thomas, G. B., Finney, R., (1988) Calculus and Analytic Geometry: 7th edition, ADDISON-WESLEY Publishing Company.
- 8- Surfer Version 9.0 (2009). Surface Mapping System. Copyright © 1993-2009, Golden Software, Inc.
- 9- Press, William H., Saul A. Teukolsky, William T. Vetterling, and Brian P. Flannery (1992) Numerical Recipes in C: The Art of Scientific Computing. Second Edition, Cambridge University Press, New York, 994 pp.
- 10- Wiggin, E., Elementary Digital Filtering: <http://www.gamedev.net/reference/articles/article1068.asp>, (09/20/2001).
- 11- Gonzalez, R. C. and Woods, R.E. (2000) Digital Image Processing: ADDISON-WESLEY. 716 P.
- 12- Weisstein, E. W. (2008). Biharmonic Equation, From MathWorld – A Wolfram Web Resource: <http://mathworld.wolfram.com/BiharmonicEquation.html>.
- 13- Carlos A. Mendonca, Ahmed M.A. Meguid. (2008). Programs to compute magnetization to density ratio and the magnetization inclination from 3-D gravity and magnetic anomalies. Computers & Geosciences. Vol. 34: No. 6: P603-610.
- 14- Banerjee, B., Das Gupta, S.P. (1977). Gravitational attraction of a rectangular parallelepiped. Geophysics. Vol. 42: No. 5: P 1053–1055.
- 15- Robert E. West (1994). The land gravity exploration method. Practical Geophysics II for the Exploration Geologist. Compiled by Richard Van Blaricom. Northwest Mining Association. P 177-233.
- 16- Pašteka, R., Richter, F.P., Karcol, R., Brada, K. and Hajach, M., (2009). Regularized derivative of potential fields and their role in semi-automated interpretation methods. Geophysical Prospecting. Vol. 57: P 507-516.

طريقة جديدة وفريدة لتحديد خصائص (ابعاد, اعماق وتباين كثافي) لاجسام موشورية ثلاثية الابعاد باستخدام المعاملات التفاضلية للانحدار, معاملات لابلاس والتوافقية المزدوجة لمجالها الجذبي .

علي مكي حسين الرحيم

E.mail: alial_rahim@yahoo.com

الخلاصة:

استخدمت المعاملات التفاضلية (الانحدار, لابلاس والتوافقية المزدوجة) لتحديد خصائص الشواذ لاجسام موشورية ثلاثية الابعاد لها اعماق وابعاد وتباين كثافي مختلف ومن خلال مجالها الجذبي المحسوب نظريا. مبدئي الانحدار ولايبلاس يستخدمان وبشكل واسع ضمن مبادئ التحليل الصوري. تقاطع المجال الجذبي مع المجالات التفاضلية المحسوبة يمكن ان تساعد في حساب العمق الى السطح العلوي للاجسام الموشورية بغض النظر عن الاختلاف في ابعادها واعماقها وتباينها الكثافي. معامل التوافقية المزدوجة اعطى نتائج ممتازة , حيث يعطي انغلاقين كنتوريين وبقيمة صفرية. حدود الانغلاق الداخلي ذي القيمة الصفرية يحدد وبصورة مضبوطة ابعاد الاجسام الموشورية. المسافة بين الكنتور الصفري والقيم العظمى لمعامل لابلاس تحدد العمق الحقيقي الى السطح العلوي للاجسام الموشورية. القيم العظمى للتوافقية المزدوجة يمكن استخدامها لتقييم التباين الكثافي. هذه هي المحاولة الاولى لاستخدام هذه الطريقة في حساب خصائص الجسم , وللمعامل التوافقي المزدوج حساسية كبيرة لظهور التراكب الصغيرة والمخفية بتأثير الاجسام القريبة والكبيرة , مرشح لابلاس لحساب المشتقة الثانية يمكنه ايضا اظهار هذه التراكب الصغيرة ولكن معامل التوافقية المزدوجة يمكنه حساب العمق المضبوط. المستخدم لهذه الطريقة يجب ان يكون حذرا خلال حساب قراءاته لكون معامل التوافقية المزدوجة حساس جدا لتغير هذه القراءات. صلاحية الطريقة اختبرت على مثال لقبة ملحية في حوض ساحل الخليج.